IOP PUBLISHING JOURNAL OF PHYSICS D: APPLIED PHYSICS

J. Phys. D: Appl. Phys. **41** (2008) 015003 (5pp) doi:10.1088/0022-3727/41/1/015003

Nanocomposite exchange-coupled magnets with two hard phases $PrCo_5C_\delta/Pr_5Co_{19}C_\varepsilon$

Bai Yang, Bao-Gen Shen[1], Tong-Yun Zhao, Hong-Wei Zhang and Ji-Rong Sun

State Key Laboratory of Magnetism, Institute of Physics and Beijing National Laboratory for Condensed Matter Physics, Chinese Academy of Sciences, Beijing 100080, People's Republic of China

E-mail: yangbai@g203.iphy.ac.cn and shenbg@g203.iphy.ac.cn

Received 8 October 2007, in final form 13 November 2007
Published 12 December 2007
Online at stacks.iop.org/JPhysD/41/015003

Abstract

Nanocomposite exchange-coupled magnets with two hard phases $PrCo_5C_\delta/Pr_5Co_{19}C_\varepsilon$ have been fabricated by melt spinning. Adding carbon is found to favour the formation of the $Pr_5Co_{19}C_\varepsilon$ phase. The exchange-coupling effect between the $PrCo_5C_\delta$ and $Pr_5Co_{19}C_\varepsilon$ phases leads to a high remanence ratio and single-phase magnetic behaviour in the ribbons. The coercivity of the $PrCo_{5-x}C_x$ ribbons increases with increasing carbon concentration. The best overall properties including a coercivity of 6.1 kOe, a remanence ratio of 0.81 and a maximum energy product of 12.0 MGOe in the ribbons with $x = 0.5$, have been obtained at room temperature.

1. Introduction

Recently, *R*-Co magnets (*R* denotes Sm or Pr) have aroused much scientific interest because they have higher Curie temperatures than $Nd_2Fe_{14}B$-based magnets, and are suitable for high-temperature applications [1–4]. $PrCo_5$ compounds show a theoretical room-temperature energy product $(BH)_{max}$ of 39 MGOe [5], about 33% higher than that of $SmCo_5$, and also it is lower in cost. Thus, much attention has been focused on the $PrCo_5$-based alloys. However, the coercivity developed in sintered [6] or melt-spun [7] Pr–Co alloys is very low (<6 kOe) as compared with the anisotropy field (145–170 kOe) of $PrCo_5$ compounds. Low coercivity is thought to be mainly due to the coarse grain structure [8,9]. It is reported that the coercivity of melt-spun Pr–Co alloys can be increased by adding carbon [10–12]. A high coercivity (>12 kOe) is achieved with high carbon levels (<6 at.%) in a Pr-rich $PrCo_5$-based alloy, but remanence loss (<5 kGs) is greater [10]. In this work, nanostructured $PrCo_5$-based $PrCo_{5-x}C_x$ ribbons with higher carbon contents (>8 at.%) have been prepared. A uniform cellular $PrCo_5C_\delta/Pr_5Co_{19}C_\varepsilon$ nanocomposite microstructure together with a high coercivity without serious sacrifice of remanence is developed in melt-spun $PrCo_{5-x}C_x$ ($x = 0.5$–0.8) ribbons. As is well known, magnetic hardening can be achieved in nanocrystalline two-phase permanent magnets containing hard and soft magnetic phases due to the exchange coupling between them [13–15]. A similar exchange hardening is found in the materials composed of two hard magnetic phases in this work. The exchange-coupling effect between the two hard phases is believed to lead to a high remanence ratio and single-phase magnetic behaviour in the ribbons. The effect of carbon addition on microstructure and magnetic properties of melt-spun $PrCo_{5-x}C_x$ ribbons is also examined.

2. Experimental approach

The alloy ingots with nominal compositions of $PrCo_{5-x}C_x$ ($x = 0$, 0.5, 0.6, 0.8 and 1) were prepared by electric arc melting the constituent materials Pr, Co and C (all with a purity of at least 99.99%) in a high-purity argon atmosphere. Pr of 5 wt% more than that of the stoichiometric value, was added to the alloys to compensate for the loss of Pr. The ribbons were obtained by melt spinning in an argon atmosphere at a wheel speed of 5–25 m s^{-1}. The phase composition of melt-spun ribbons was examined by x-ray diffraction (XRD) using Cu Kα radiation. Microstructural studies were carried

[1] Author to whom any correspondence should be addressed.

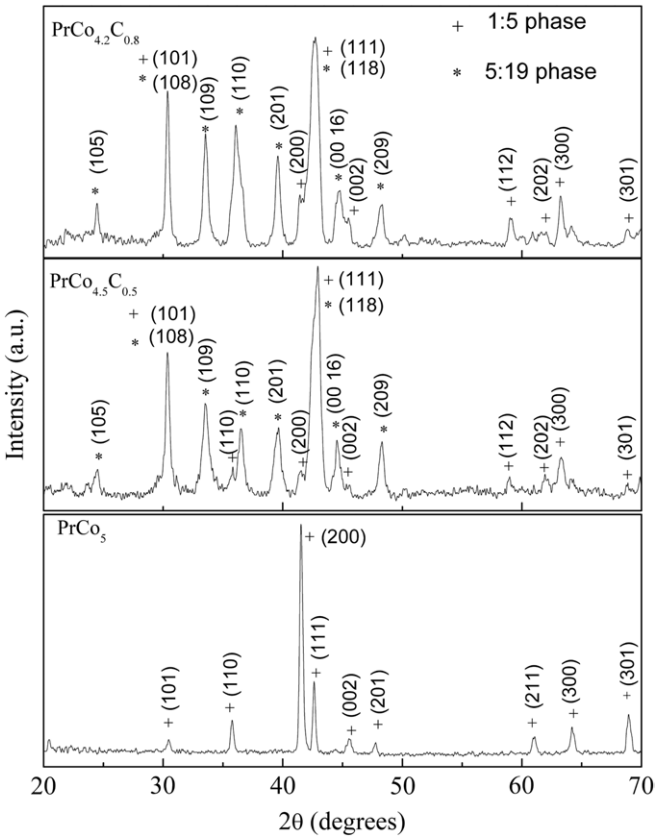

Figure 1. XRD patterns of melt-spun $PrCo_5$ ribbons prepared at 5 m s^{-1} and the $PrCo_{5-x}C_x$ ($x = 0.5$ and 0.8) ribbons spun at 25 m s^{-1}.

out using a JEOL JEM-2010 transmission electron microscope (TEM). The energy dispersive spectroscope (EDS) was used to determine the chemical contents of the elements in the ribbons. The EDS measurements were operated with electron energy of 0–40 keV and the measurement errors were within 2% of the average chemical contents of the elements. Thermomagnetic measurements were performed by using a vibrating sample magnetometer (VSM) in a temperature range 25–800 °C under an applied field of 1 kOe. The hysteresis loops were measured by a superconducting quantum interference device (SQUID) in applied fields of 20–50 kOe at room temperature.

3. Results and discussion

Figure 1 displays the XRD patterns of melt-spun $PrCo_5$ ribbons prepared at 5 m s^{-1} and the $PrCo_{5-x}C_x$ ($x = 0.5$ and 0.8) ribbons spun at 25 m s^{-1}. The carbon-free ribbons exhibit a nearly pure 1 : 5 phase ($CaCu_5$ structure) with a strong (2 0 0) texture, similar to the structure observed from $SmCo_5$ ribbons melt spun at 5 m s^{-1} [16]. The XRD patterns for $PrCo_{5-x}C_x$ ribbons with $x = 0.5$ and 0.8 melt spun at 25 m s^{-1} are different from those for carbon-free ribbons. It can be seen from figure 1 that the (2 0 0) reflections of the 1 : 5 phase in $PrCo_{5-x}C_x$ ($x = 0.5$ and 0.8) are very weak as compared with those of carbon-free ribbons. No texture for carbon-addition ribbons is observed, indicating that the two carbides show an isotropic characteristic. Figure 2 illustrates the temperature

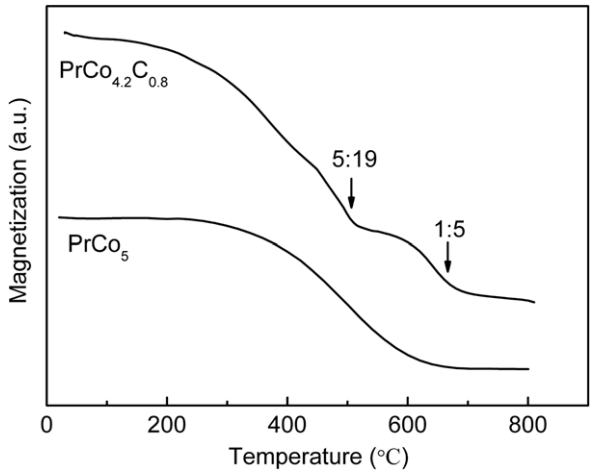

Figure 2. Temperature dependences of magnetizations of $PrCo_5$ and the ribbons with $x = 0.8$ under an applied field of 1 kOe.

dependence of magnetization of melt-spun ribbons with $x = 0$ and 0.8 under an applied field of 1 kOe. For the ribbons with $x = 0.8$, besides the onset at 680 °C corresponding to the 1 : 5 phase, an onset at about 500 °C is observed, indicative of the existence of another magnetic phase in the ribbons. According to four characteristic peaks near $2\theta = 24°$, 33°, 36° and 39° in the XRD patterns, the existence of the 5 : 19 phase is determined in the ribbons with $x = 0.5$–0.8 by the structural comparisons with the known binary Pr–Co compounds (including $PrCo_2$, $PrCo_3$, $PrCo_7$, Pr_2Co_{17}, Pr_4Co_3, Pr_5Co_{19} and Pr_2Co_7) and the ternary Pr–Co–C compounds (including $PrCoC_2$ and $Pr_3Co_4C_x$). The lattice constants of the 1 : 5 phase ($a = 0.5067$ nm, $c = 0.4030$ nm) in the ribbons with $x = 0.8$ are about 0.8% larger than those of a pure $PrCo_5$ ($a = 0.5027$ nm, $c = 0.3988$ nm). Meanwhile, the lattice constants for the 5 : 19 phase ($a = 0.5114$ nm, $c = 3.2916$ nm) are also larger than those of a pure Pr_5Co_{19} ($a = 0.5054$ nm, $c = 3.2430$ nm). The lattice expansion suggests that carbon atom enters the interstitial positions of the $PrCo_5$ and Pr_5Co_{19} phases. Furthermore, as shown in figure 2, the Curie temperatures of $Pr_5Co_{19}C_\varepsilon$ and $PrCo_5C_\delta$ (500 and 680 °C) both are higher than those of the corresponding carbon-free compounds (417 and 620 °C) [17], which may be caused by the lattice expansion due to the carbon addition and the change of compositions of the two phases with and without carbon.

The R_5Co_{19} phase is formed from RCo_5-based alloy by eutectoid decomposition for R = La, Ce, Pr and Nd; the Pr_5Co_{19} phase often appears in sintered $PrCo_5$-based permanent magnets [17, 18]. It is difficult to form a single Pr_5Co_{19} phase in binary or ternary Pr–Co alloys prepared even under the nonequilibrium processing such as mechanical milling [19] and rapid solidification [11]. Instead, a successive heat treatment can lead to the appearance of the Pr_5Co_{19} phase [20]. In our experiments, the $Pr_5Co_{19}C_\varepsilon$ phase is formed in Pr–Co–C alloys by direct melt spinning, which shows that adding a large amount of carbon is helpful to the formation of Pr_5Co_{19} phase. The Pr_5Co_{19} compound has a crystal structure of hexagonal symmetry, the same as that of $PrCo_5$ compound. But the interstitial volume of the Pr_5Co_{19} phase is much larger

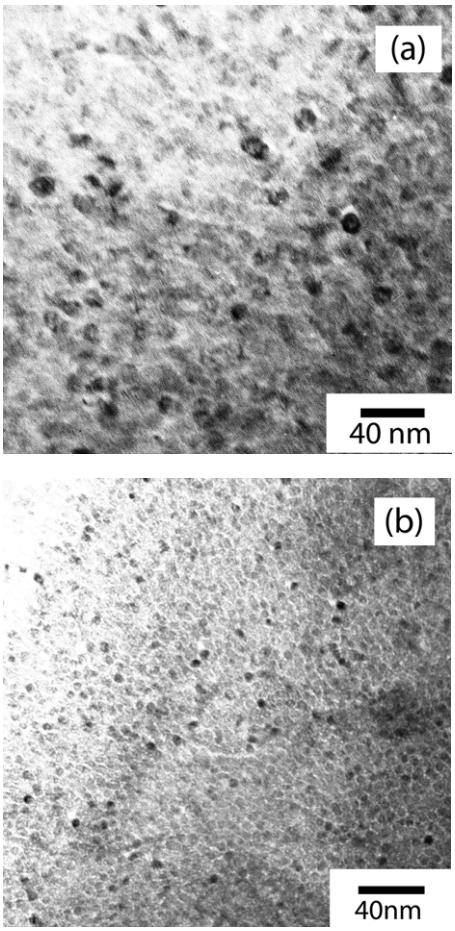

Figure 3. TEM micrographs of the ribbons with $x = 0.5$ (*a*) and 0.8 (*b*) prepared at an optimum wheel speed of 25 m s^{-1}.

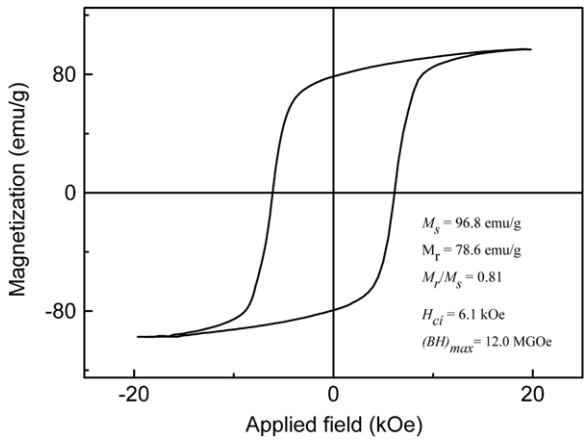

Figure 4. Room-temperature hysteresis loop of the ribbons with $x = 0.5$.

than that of $PrCo_5$ because of their lattice constants. It means that much more interstitial carbon atoms can dissolve into Pr_5Co_{19} lattice. Our further experiment shows that the ribbons with $x = 1$, i.e. much more carbon contents, are composed of Pr_2C_3 and Co, and a small amount of the 1 : 5 phase.

Figure 3 shows the representative TEM micrographs of the ribbons with $x = 0.5$ and 0.8 prepared at an optimum wheel speed of 25 m s^{-1}. A uniform cellular $PrCo_5C_\delta/Pr_5Co_{19}C_\varepsilon$ microstructure is found in figure 3. The average atomic ratios of Pr : Co : C obtained by EDS for the matrix phase and the grain boundary phase are 16.3 : 81.1 : 2.6 and 21.3 : 74.9 : 4.8, respectively. The ratios of Pr : Co approach the 1 : 5 and 5 : 19 phases for the matrix phase and the grain boundary phase, respectively, which is further evidence for the existence of the 5 : 19 phase in the ribbons with $x = 0.5$–0.8. The grain of the $PrCo_5C_\delta$ phase in the ribbons is surrounded by a 2 nm wide grain boundary phase. The grain size of the $PrCo_5C_\delta$ phase is about 5–15 nm. As shown in figure 3, a much more homogeneous microstructure with finer grains is observed as the carbon content increases from 0.5 to 0.8.

Figure 4 shows the typical room-temperature hysteresis loop of $PrCo_{4.5}C_{0.5}$ ribbons measured under a maximum magnetic field of 20 kOe. Strong intergrain exchange coupling is revealed by a remanence ratio of 0.81 larger than 0.5 predicted by the Stoner–Wohlfarth theory for noninteraction single-domain particle assembly. Additionally, the smooth demagnetization curves, as expected by a magnet with a magnetic single phase, indicate that the magnetic behaviours of the $PrCo_5C_\delta$ and $Pr_5Co_{19}C_\varepsilon$ phases are exchange coupled. Our investigations find that there exists an intergrain exchange coupling between the $PrCo_5C_\delta$ and $Pr_5Co_{19}C_\varepsilon$ phases in the samples with $x = 0.5$–0.8.

The exchange interactions between the grains in nanocomposite magnets [21] can be qualitatively verified by a Henkel plot, which is expressed as

$$\delta m(H) = [M_d(H) - M_r + 2M_r(H)]/M_r, \qquad (1)$$

where $M_r(H)$ is the remanent magnetization acquired after the application and subsequent removal of a direct field H, and $M_d(H)$ is dc demagnetization remanence after dc saturation in one direction and the subsequent application and removal of the direct field in the reverse direction. The positive $\delta m(H)$ peak height in the Henkel plot indicates the existence of exchange coupling between the two kinds of phases in nanocomposite magnets [22]. For the $PrCo_{5-x}C_x$ ribbons with $x = 0.5$ and 0.8, larger positive values of $\delta m(H)$ at the field slightly less than coercivity are observed, as shown in figure 5, indicating the existence of exchange-coupling interactions between the $PrCo_5C_\delta$ and $Pr_5Co_{19}C_\varepsilon$ phases in two nanostructured ribbons. The maximum value of $\delta m(H)$ for $PrCo_{5-x}C_x$ ribbons with $x = 0.5$ is higher than that of the ribbons with $x = 0.8$, which reflects the stronger intergrain exchange coupling [23] in nanostructured $PrCo_{4.5}C_{0.5}$ ribbons. Estimating by XRD patterns in figure 1 and TEM micrographs in figure 3, it can be seen that the volume fraction of the $Pr_5Co_{19}C_\varepsilon$ phase increases from about 12% to 22% with x increasing from 0.5 to 0.8. The decrease in intergrain exchange coupling for $PrCo_{5-x}C_x$ ribbons with increasing content of the $Pr_5Co_{19}C_\varepsilon$ phase is similar to the results observed in nanocomposite magnets consisting hard and soft magnetic phases, in which the intergrain exchange coupling decreases with increasing the soft phase content [24].

Figure 6 summarizes room-temperature saturation magnetization M_s, remanence ratio M_r/M_s, coercive field H_{ci} and maximum energy product $(BH)_{max}$ as functions of x for

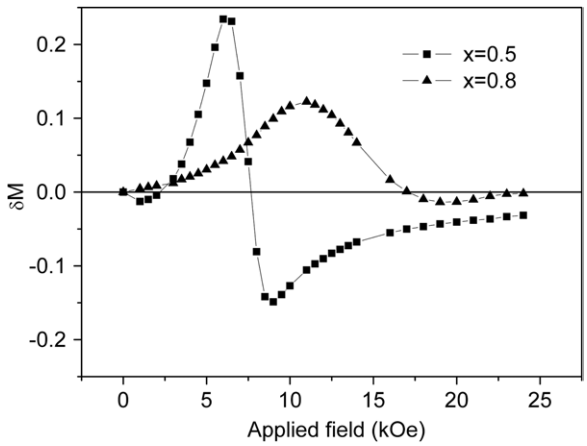

Figure 5. The variations of δM with applied field of $PrCo_{5-x}C_x$ ($x = 0.5$, 0.8) ribbons melt spun at 25 m s^{-1}.

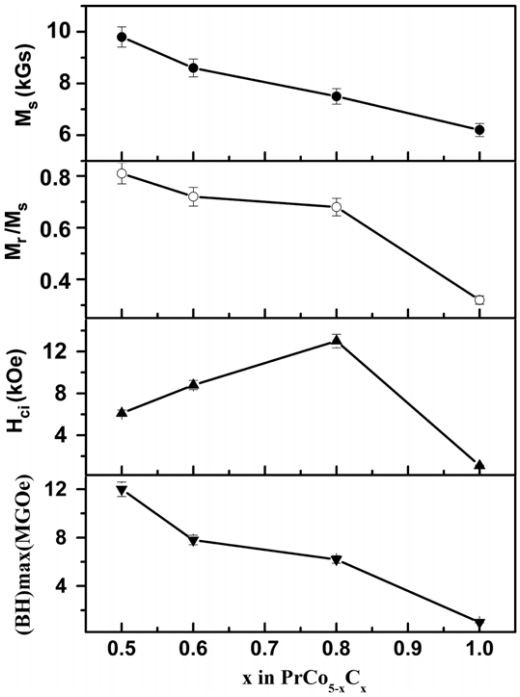

Figure 6. Room-temperature coercive field H_{ci}, saturation magnetization M_s, remanence ratio M_r/M_s and maximum energy product $(BH)_{max}$ as functions of C content x for $PrCo_{5-x}C_x$ ($x = 0.5$, 0.6, 0.8, 1) ribbons prepared at 25 m s^{-1}.

the ribbons prepared at 25 m s^{-1}. The values of M_s and M_r/M_s decrease with the increase in x, which is due to magnetic dilute effect of carbon addition. The coercivity of the ribbons increases from 6.1 to 13.0 kOe with the increase in x from 0.5 to 0.8, and then drops off rapidly for $x = 1$. The magnetic hardening of the ribbons with $x = 0.5$–0.8 can be ascribed to the exchange-coupling effect between $PrCo_5C_\delta$ and $Pr_5Co_{19}C_\varepsilon$ phases due to the fineness of grain and uniform nanometric microstructure. Although $Pr_5Co_{19}C_\varepsilon$ is a magnetically hard phase, its anisotropy field (38 kOe) [17] is much lower than that of $PrCo_5$ (170 kOe). The nanometric $PrCo_5C_\delta/Pr_5Co_{19}C_\varepsilon$ grains with uniform distribution lead to intergranular exchange coupling between them. This is believed to be the main reason for high coercivity obtained in $PrCo_{5-x}C_x$ ribbons ($x = 0.5$–0.8) with the existence of the 5 : 19 phase, which often appears as the detrimental impurity phase in sintered $PrCo_5$-based magnets. The increasing of coercivity with the increase in carbon content is mainly due to the refinement of grain size as shown in figure 3. For $x = 1$, the formation of Pr_2C_3 and Co results in a dramatic decrease in coercivity. The coercivity reaches a maximum of 13.0 kOe with $x = 0.8$, but the maximum energy product is lower due to its low remanence. The best magnetic properties including a coercivity of 6.1 kOe, a remanence of 7.9 kGs and a maximum energy product of 12.0 MGOe in the ribbons with $x = 0.5$ have been obtained at room temperature.

4. Conclusions

In summary, for the $PrCo_{5-x}C_x$ ($x = 0.5$–0.8) ribbons fabricated by direct melt spinning, carbon addition is found to favour the formation of the $Pr_5Co_{19}C_\varepsilon$ phase. A uniform cellular $PrCo_5C_\delta/Pr_5Co_{19}C_\varepsilon$ nanocomposite microstructure is developed in the ribbons. The coercivity of the ribbons reaches a maximum of 13.0 kOe for $x = 0.8$. The best room-temperature magnetic properties including a coercivity of 6.1 kOe, a remanence ratio of 0.81 and a maximum energy product of 12.0 MGOe in the ribbons with $x = 0.5$ have been obtained. The magnetic hardening of nanocomposite $PrCo_5C_\delta/Pr_5Co_{19}C_\varepsilon$ ribbons is believed to arise from intergranular exchange coupling between the two phases.

Acknowledgments

This work was supported by the National Nature Science Foundation of China and the National Basic Research Program of China.

References

[1] Pedziwiatr A T, Sankar S G and Wallace W E 1988 *J. Appl. Phys.* **63** 3710
[2] Ido H, Konno K, Cheng S F, Wallace W E and Sankar S G 1990 *J. Appl. Phys.* **67** 4638
[3] Yan A R, Zhang W Y, Zhang H W and Shen B G 2000 *J. Appl. Phys.* **88** 2787
[4] Aich S, Ravindran V K and Shied J E 2006 *J. Appl. Phys.* **99** 08B521
[5] Velu E M T, Obermyer R T, Sankar S G and Wallace W E 1989 *J. Less-Common Met.* **148** 67
[6] Wallace W E, Craig R S, Gupta H O, Hirosawa S, Pedziwiatr A, Oswald E and Schwab E 1984 *IEEE Trans. Magn.* **20** 1599
[7] Fuerst C D and Brewer E G 1993 *J. Appl. Phys.* **74** 6907
[8] Chen Z M, Burany X M and Hadjipanayis G C 1999 *Appl. Phys. Lett.* **75** 3165
[9] Branagan D J, Kramer M J, Tang Y L and McCallum R W 2000 *J. Appl. Phys.* **87** 6737
[10] Fuerst C D, Herbst J F, Murphy C B and Van Wingerden D J 1993 *J. Appl. Phys.* **74** 4651
[11] Lewis L H, Bian W M, Zhu Y and Welch D O 1996 *J. Appl. Phys.* **79** 351

[12] Zhao X G, Zhang Z D, Yao Q, Wen W J, Liu J J, Liu W and Geng D Y 2007 *J. Alloys Compounds* **427** 209
[13] Coehoorn R, Mooij D B and Waard C DE 1989 *J. Magn. Magn. Mater.* **80** 101
[14] Kneller E F and Hwaig R 1991 *IEEE Trans. Magn.* **27** 3588
[15] Skomski R and Coey J M D 1993 *Phys. Rev.* B **48** 15812
[16] Zhang W Y, Shen B G, Cheng Z H, Li J Q, Li L and Zhou Y Q 2001 *Appl. Phys. Lett.* **79** 1843
[17] Ray A E and Strnat K J 1975 *IEEE Trans. Magn.* **MAG-11** 1429
[18] Strnat K J, Ray A E and Mildrum H F 1977 *IEEE Trans. Magn.* **MAG-13** 1323
[19] Chen Z M, Zhang Y and Hadjipanayis G C 2000 *J. Appl. Phys.* **88** 1547
[20] Kostogorova J and Shield J E 2006 *J. Appl. Phys.* **99** 08B514
[21] Chen Q, Ma B M, Lu B, Huang M Q and Laughlin D E 1999 *J. Appl. Phys.* **85** 5917
[22] Fearon M, Chantrell R W and Wohlfarth E P 1990 *J. Magn. Magn. Mater.* **86** 197
[23] Zhang H W, Rong C B, Du X B, Zhang J, Zhang S Y and Shen B G 2003 *Appl. Phys. Lett.* **82** 4098
[24] Panagiotopoulos I, Withanawasam L and Hadjipanayis G C 1996 *J. Magn. Magn. Mater.* **152** 353